

## CHAPTER VI

### STUDY TO SYNTHESIZE AND CHARACTERIZE HOST-GUEST ENCAPSULATION OF ANTIDIABETIC DRUG (TGC) AND HYDROXY PROPYL- $\beta$ -CYCLODEXTRIN AUGMENTING THE ANTIDIABETIC APPLICABILITY IN BIOLOGICAL SYSTEM

---

#### ABSTRACT

An inclusion complex of a biologically active alkaloid Trigonelline hydrochloride (TgC) and hydroxypropyl- $\beta$ -cyclodextrin (HP- $\beta$ -CD) was prepared and characterized by several physicochemical and spectroscopic methods. The Trigonelline/HP- $\beta$ -CD inclusion complex was confirmed by UV-vis Job's plot, fluorescence, conductance and SEM. Here, the inclusion mode is described with regard to structural aspect using  $^1\text{H}$  NMR, FTIR spectroscopy. Trigonelline hydrochloride (TgC) being an anti diabetic natural product, its inclusion complex was precisely checked for its sustained release by fluorescence spectroscopy.

**Keywords:** Trigonelline Hydrochloride (TgC), hydroxypropyl- $\beta$ -Cyclodextrin (HP- $\beta$ -CD), Scanning Electron Microscope (SEM), Encapsulation, NMR, Fluorescence.

#### 1. Introduction:

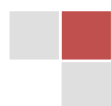
Fenugreek (*Trigonella foenum graecum*) is one of the most widely used medicinal plants in medicine. Trigonelline hydrochloride (TgC), one of the major alkaloid of fenugreek, has been reported to be responsible for showing immense potential pharmacological activities. It has the ability to reduce blood glucose concentration in rats [1, 2] and in human [3,4] which indicate that it has a potential antidiabetic activity. It helps to reduce the total cholesterol (TC) and triglyceride (TG) levels. TgC has antioxidant activities in cell-free systems as well as human colon cell lines [5]. The anti diabetic activity of the fenugreek seeds have been reported [6]. It protects  $\beta$ -cells of the pancreas and increases insulin sensitivity index as well as insulin content [7].



Cyclodextrins (CDs) are cyclic oligo saccharides of  $\alpha$ -D-glucose that are formed through glycosidic  $\alpha$ -1, 4 bonds [8]. Cyclodextrins (CDs) have been used extensively as additives that can increase the solubility of poorly water-soluble organic compounds, by forming an inclusion complex between the host cyclodextrin and the guest molecules [9]. The resulting inclusion or host-guest complexes having unusual physical, chemical and biological properties can greatly increase the interest in scientific and technological aspect, e.g, inner cavity of Cyclodextrins are hydrophobic whereas outer cavity is hydrophilic in nature [10]. Such noncovalent interactions can actually improve the guest's water solubility, bioavailability as well as stability [11]; they can also be used for controlled release of the guest molecules [12]. Hydroxypropyl-beta-cyclodextrin (HP- $\beta$ -CD), a hydroxy alkyl derivative, is an alternative to parent CDs, having higher water solubility and may have slightly more toxicologically benign [13]. 2-hydroxy propyl- $\beta$ -cyclodextrin is commercialised under the trade name of Molecusol™ and Encapsin™ [14]. It does not have any nephrotoxicity in human body just like beta-cyclodextrin. As the first approved CD derivative by FDA, HP- $\beta$ -CD has wide applications in food, pharmaceuticals and agriculture etc [15].

In order to show some therapeutic affect on biological system, a drug has to be released from their carrier. Here, cyclodextrin has been used as the drug carrier. From the literature, it is reported that hydroxy propyl- $\beta$ -cyclodextrin can be used modified or controlled release carrier.

In the present study, HP- $\beta$ -CD has been used as the host molecule whereas TgC as guest molecule. HP- $\beta$ -CD can increase the water solubility of pure TgC (50mg/mL) to up to four times after formation of the inclusion complex (196mg/mL) and hence increase the bio availability of the drug. It will also be studied that whether the inclusion complex show sustained release or not. In this aspect, fluorescence spectroscopy will be involved as the measurement.



## 2. Materials and Methods:

### 2.1. Materials:

Trigonelline hydrochloride (Molecular weight = 173.60 g/mol, Purity > 98%) used in this work was purchased from Sigma Aldrich. 2-Hydroxypropyl- $\beta$ -cyclodextrin (HP- $\beta$ -CD, average molecular weight = 1541.54 g/mol) was obtained from TCI chemicals India PVT. LTD and used without further purification. Other reagents and chemicals were of analytical reagent grade. All experiments were done using double distilled water.

### 2.2. Methods:

#### 2.2.1 Preparation of TgC/HP- $\beta$ -CD inclusion complex:

An inclusion complex of TgC/HP- $\beta$ -CD was prepared in 1:1 molar ratio by simple co-precipitation method [16]. First, TgC (25 mg) and HP- $\beta$ -CD (225.89 mg) were dissolved in minimum volume of pure distilled water, then the two solutions were mixed in a 50 ml beaker and kept at 50°C with stirring of 350 rpm/min for 24 hours. Finally, the sample was evaporated under reduced pressure in a rotary evaporator at 40 to produce a solid inclusion complex.

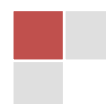
#### 2.2.2 Preparation of physical Mixture:

A physical mixture of TgC and HP- $\beta$ -CD with a 1:1 molar ratio was also prepared by mixing solid TgC and HP- $\beta$ -CD thoroughly for 10 min in a ceramic mortar unless a homogeneous mixture was obtained. [17]

### 2.3 Inclusion Complex characterization:

#### 2.3.1 UV measurement:

UV spectra of the inclusion complex, TgC and HP- $\beta$ -CD were obtained by Agilent 8453 UV-vis spectrophotometer with uncertainty  $\pm 2$  nm. A conventional 1



cm path (1 cm × 1 cm × 4 cm) quartz cell has been used. UV instrument was attached with a digital thermostat. The scans were taken within range from 190 to 1200 nm.

As the compound TgC was water soluble, double distilled H<sub>2</sub>O had been used for the spectral measurements [18].

### 2.3.2 Conductance:

Conductance measurements were taken in SYSTRONICS CONDUCTIVITY-TDS METER 308 instrument [19]. Prior to the experiment, cell constant and specific conductance of the solvent (H<sub>2</sub>O) were measured. Cell constant was found to be 0.10 cm<sup>-1</sup>. Specific Conductance of 10 mM, 10 mL pure TgC was 18.2 mScm<sup>-1</sup>.

### 2.3.3 Fourier Transform Infrared Spectroscopy (FT-IR):

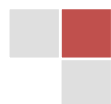
The FT-IR analysis was performed on a Perkin Elmer Spectrum FT-IR spectrometer, using KBr pellets [20]. The samples of TgC, HP-β-CD, physical mixture, and their inclusion complex were previously ground and mixed thoroughly with KBr. The KBr disks were prepared by compressing the powder. The scans were done with a resolution of 4 cm<sup>-1</sup>, from 4000 to 500 cm<sup>-1</sup>. The concentration of the sample in pellets was 1 mg/100 mg KBr [20].

### 2.3.4 <sup>1</sup>H NMR:

One-dimensional <sup>1</sup>H NMR spectra were recorded at room temperature on Bruker AVANCE III 400 NMR spectrometer. TgC, HP-β-CD and the complex TgC/HP-β-CD were respectively dissolved in D<sub>2</sub>O (Aldrich). The signal at 4.67 ppm of HOD was used as an internal reference [21].

### 2.3.5 Scanning electron microscope (SEM):

The surface morphologies of TgC, HP-β-CD, TgC/ HP-β-CD physical mixture and TgC/ HP-β-CD inclusion complex were determined by JEOL JSM-IT 100 scanning electron microscope [22]. The pictures were taken at an excitation voltage of 15, 20 or 30 kV and a magnification of 425, 500, 1000 or 2000×.



### 2.3.6 Sustained release by Fluorescence:

Release kinetics was studied with the help of fluorescence spectroscopy to determine the variation in maximum emission intensity with time [23]. First, 100  $\mu\text{M}$  solution of inclusion complex (TgC/HP- $\beta$ -CD) was prepared in Double distilled water. Excitation of the fluorescence spectrometer was set at 265 nm, emission scan was adjusted in the range of 275-650 with slit width at 2 nm and spectra were recorded with time gap of 0, 10, 20, 30, 40, 60, 75, 90, 105, 150, 210mins.

## 3. Results and discussion:

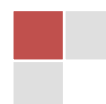
### 3.1 Job-plot by UV-vis determination:

The stoichiometry of inclusion complex was determined by the continuous variation Job's method [24]. First, 100  $\mu\text{M}$  solution of both TgC and HP- $\beta$ -CD were prepared and then they were mixed by varying the molar ratio (4 mL:0 mL, 3.6mL:0.4mL, 3.2 mL:0.8 mL and so on) but the total concentration of the species were kept constant. After 1 hour, the absorbance at  $\lambda_{\text{max}}$  was determined for all the solutions and the difference in absorbance in the presence and in absence of HP- $\beta$ -CD was plotted against R ( $R = [\text{TgC}]/\{[\text{TgC}]+[\text{HP-}\beta\text{-CD}]\}$ ). The shift of  $\lambda_{\text{max}}$  around 265 nm of the UV-spectrum of TgC was observed to prepare the Job's plot. The absorption peak observed at 265 nm for TgC in water was due to the  $\Pi$ - $\Pi^*$  transition of the pyridinium moiety. The Fig. 1 shows a maximum value at  $r = 0.50$ , corresponding to 1:1 (TgC: HP- $\beta$ -CD) stoichiometry.

### 3.2 Association constant calculation by UV-vis measurement:

Association constant and stoichiometric ratio of the inclusion complex TgC/HP- $\beta$ -CD can be calculated according to the Benesi-Hindebrand double reciprocal plot assuming the formation of a 1:1 host-guest complex [25].

$$\frac{1}{\Delta A} = \frac{1}{K[\text{TgC}]\Delta\epsilon} \times \frac{1}{[\text{HP}\beta\text{CD}]} + \frac{1}{[\text{TgC}]} \dots (1)$$



Where,  $\Delta A$  is the difference of absorbance between the TgC in the absence and presence of the HP- $\beta$ -CD at a particular wavelength,  $\Delta \epsilon$  is the difference in the molar absorptivities between guest (TgC) and inclusion complex. The Fig. 2 showed the variation in UV-vis spectral changes of TgC on addition of different strength of solution.

Plot of  $1/\Delta A$  versus  $1/[HP-\beta-CD]$  for three different temperatures (293K, 298K, 303K) had been taken and was found to be straight lines (Fig S1 in supporting information). Linear correlation was satisfactory ( $R^2= 0.661$  at 293k,  $R^2= 0.891$  at 298k,  $R^2= 0.999$  at 303k), which is less than 1, it's also confirm that the formation of a 1:1 encapsulation complex.

From the intercept and slope of these plot, association constant ( $K_a$ ) was found to be  $-141005 \text{ M}^{-1}$  at 293K,  $-69976 \text{ M}^{-1}$  at 289K,  $-8416 \text{ M}^{-1}$  at 303K. Decrease in the negative  $K_a$  value with temperature was likely due to the weakening of the intermolecular forces such as van der Waals or hydrogen bonding forces and as the temperature was raising binding between guest (TgC) and host (HP- $\beta$ -CD) became more powerful.

The change in Gibbs' free energy ( $\Delta G$ ) for the inclusion process was calculated according to the given equation.

$$\Delta G = \Delta H - T\Delta S \dots (2)$$

From the Van't Hoff equation, enthalpy Change ( $\Delta H$ ) and entropy Change ( $\Delta S$ ) can be easily obtained [26].

$$\ln K = -\frac{\Delta H}{RT} + \frac{\Delta S}{R} \dots (3)$$

Parameters have been shown in the Table 1. There are various binding forces involved during the inclusion phenomena such as hydrogen bonds, electrostatic interactions, hydrophobic forces and van der Waals interactions.



According to Ross and Subramanian [27], various thermodynamic rules can be used to interpret the type of binding mode which is summarized below:

- (a)  $\Delta H > 0$  and  $\Delta S > 0$  i.e., hydrophobic forces;
- (b)  $\Delta H < 0$  and  $\Delta S > 0$  i.e., electrostatic interactions;
- (c)  $\Delta H < 0$  and  $\Delta S < 0$  i.e., van der Waals interactions and hydrogen bonds.

In our case, we got positive  $\Delta H$  and  $\Delta S$  suggest that inclusion process was endothermic in nature and hydrophobic forces played an important role to favour the inclusion complex, again, slight negative  $\Delta G$  value suggest that interaction between TgC and HP- $\beta$ -CD was spontaneous [28].

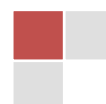
### 3.3 Association Constant measurement by fluorescence measurement:

The association constant can also be determined by monitoring the Changes in fluorescence emission due to the interaction between any guest and host molecules [29, 30]. In case of fluorescence measurement to calculate the association constant, modified Stern–Volmer equation has been used.

$$\frac{F_0}{\Delta F} = \frac{1}{f \cdot K_a} \times \frac{1}{[Q]} + \frac{1}{f} \dots \text{(4)}$$

Where,  $\Delta F$  is the difference in fluorescence in the absence and presence of the cyclodextrin at a concentration  $[Q]$ ,  $f$  is the fraction of accessible fluorescence, and  $K_a$  is the effective quenching constant for the accessible fluorophores, which are analogous to the associative binding constants for the host-guest system. According to the above equation, the binding constants  $K_a$  can be obtained by plotting  $F_0/\Delta F$  vs.  $1/[Q]$  and the results are shown below. TgC showed a linear fit curve when complexed with HP- $\beta$ -CD that indicates 1:1 binding stoichiometry.

The variation in the fluorescence emission spectra were given in the Fig. 3 and the plot were given in Fig. S3 in supporting information. The spectra were scanned in the UV–VIS spectral range (275–650 nm) by exciting at 265 nm with scanned speed at 1 nm/sec and slit width at 2 nm. The fluorescence emission

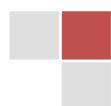


maxima were found at four different bands located in the spectral ranges 275-300, 375-500, 515-550 and 550-600 nm. The fluorescence emission peak found at 433 nm was due to the corresponding emission of the  $\pi \rightarrow \pi^*$  transition of the pyridinium moiety [31]. The other peaks were probably due to the solvent and host molecules present in the solution. The association constant have been calculated with different concentration of solution at 433 nm.

According to the Benesi-Hildebrand (B-H) method, it was found to be 1:1 stoichiometric ratio. Further, to verify the association constant values, a modified Stern–Volmer equation can be used to determine the value of  $K_a$  and it was found to be around  $-5000 \text{ M}^{-1}$  which was quite comparable with the data obtained in UV-vis spectroscopy at  $30^\circ\text{C}$ .

### 3.4 Conductance Measurements:

Conductometric method is one of the older but precious methods used to validate not only the inclusion process between guests and the host but also stoichiometry of the inclusion complex [32]. The conductivity curve has been shown in the Fig. 4 and the conductance values have been provided in table 5 of supporting information. Prior to the experiment, 10 mM of the guest (TgC) as well as host (HP- $\beta$ -CD) were prepared using  $\text{H}_2\text{O}$  as solvent. Then, 10 ml pure TgC aliquot was taken and its conductivity was measured, it was found to be  $18.2 \text{ mSm}^{-1}$ . When, 1 ml of the HP- $\beta$ -CD was added to the 10 ml of the guest solution, conductivity was found to be decreased gradually. The decreasing conductivity with adding HP- $\beta$ -CD concentration, demonstrating the inclusion-complex formation between HP- $\beta$ -CD and the TgC. After a certain concentration, the linearly decreasing tendency was going slow down with the addition of HP- $\beta$ -CD. A distinct breakpoint was found out in the conductivity curve at a concentration of about 6 mM suggesting that the Complexation was equimolar as concentration ratio between HP- $\beta$ -CD and TgC was 1.5. This indicates that either TgC was almost totally bounded in the cavity of the HP- $\beta$ -CD or TgC was completely encapsulated by HP- $\beta$ -CD by means of non-covalent interactions.



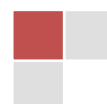
### 3.5 IR analysis:

Fourier Transform Infrared spectroscopy (FT-IR) is an important method used to validate the formation of an inclusion complex [33]. The FT-IR spectra of TgC, HP- $\beta$ -CD, TgC/ HP- $\beta$ -CD physical mixture, TgC/HP- $\beta$ -CD inclusion complex are shown in Fig. 5. The variations in stretching frequency after inclusion complex formation were shown in Table 3. The FT-IR spectrum of TgC consisted of the absorption bands of O-H group of  $-\text{COOH}$  ( $3410\text{ cm}^{-1}$ ). In the region of  $3084\text{--}3040\text{ cm}^{-1}$ , the stretching frequency of C-H from  $-\text{CH}_3$  and  $\text{C}_{\text{sp}^2}\text{-H}$  from aromatic ring appeared. C=O group of the  $-\text{COOH}$  appears at  $1711\text{ cm}^{-1}$ .

A strong absorption at  $2357\text{ cm}^{-1}$  is may be due to the presence of C=N bond in pyridinium moiety. The absorption peak in  $1469\text{ cm}^{-1}$  is corresponding to the C=C stretching vibration in the aromatic ring.

The FT-IR spectrum of HP- $\beta$ -CD showed significant absorption bands at  $3410\text{ cm}^{-1}$  (for O-H stretching vibrations),  $2928\text{ cm}^{-1}$  (for  $\text{C}_{\text{sp}^3}\text{-H}$  stretching vibrations) and  $1373\text{ cm}^{-1}$  (C-H stretching vibration from  $\text{CH}_3$ ).

However, in case of both the physical mixture and inclusion complex, the absorption band between  $3084\text{--}3040\text{ cm}^{-1}$  disappears which indicate that C-H from  $-\text{CH}_3$  and  $\text{C}_{\text{sp}^2}\text{-H}$  from aromatic ring may be inserted into the cavity of the cyclodextrin moiety. O-H stretching frequency from  $-\text{COOH}$  in TgC is  $3414\text{ cm}^{-1}$  which is shifted towards lower region at  $3410\text{ cm}^{-1}$  and  $3400\text{ cm}^{-1}$  for TgC/HP- $\beta$ -CD inclusion complex and physical mixture respectively, this is may be due to the formation of H-bonding with host moiety. A peak appeared at  $1711\text{ cm}^{-1}$  for  $-\text{COOH}$  in pure TgC had shifted to  $1723\text{ cm}^{-1}$  in case of inclusion complex may be due to intermolecular hydrogen bond between OH of  $-\text{COOH}$  and terminal secondary hydroxyl group of the HP- $\beta$ -CD. However, the peak appeared at  $1701\text{ cm}^{-1}$  in case of physical mixture which indicates that guest molecule was present outside the cavity of cyclodextrin molecules. The band at  $1469$  and  $1391\text{ cm}^{-1}$  which is generally due to C=C double bond from pyridine moiety diminished after formation of the encapsulated complex.



According to these changes, we might suggest that the pyridinium ring of TgC was committed.

### 3.6 $^1\text{H-NMR}$ analysis:

NMR (Nuclear Magnetic Resonance) is one the most powerful instrument in the study of CD complexes which provides quantitative information on spatial arrangement in case of 2D-NMR as well as detailed information on the possible inclusion mode in case of  $^1\text{H-NMR}$  of CD with guest molecules [34].

Fig. 6 shows the change in chemical shift of the TgC after the formation of inclusion complex. Fig. 7 shows the chemical shifts of TgC, HP- $\beta$ -CD, TgC/HP- $\beta$ -CD inclusion complex and their variation in the chemical shift ( $\Delta\delta$ ) of the complex. After the formation of inclusion complex with TgC, the H-3 proton of HP- $\beta$ -CD shifted 0.04 ppm and the H-5 proton of HP- $\beta$ -CD shifted 0.01 ppm (Table 4). In case of the  $^1\text{H-NMR}$ , if the guest moiety TgC enters into the cavity of the HP- $\beta$ -CD molecules, electron density over the H-3, H-5 proton will be increased as both H-3 and H-5 protons are located in the inner part of the HP- $\beta$ -CD cavity and consequently it will shield the protons and induce upfield shift. Again, chemical shift of the pyridinium moiety after inclusion has been shifted to lower (upfield) region that may be due to the van der Waals interaction. All these data leads to the confirmation that TgC had an interaction with the cyclodextrin cavity.

### 3.7 SEM analysis:

Scanning electron microscope (SEM) is a qualitative technique used to study the change in the surface morphology of different materials like other high resolution microscopic technique [35, 36]. SEM photographs of (a) TgC, (b) HP- $\beta$ -CD, (c) TgC/HP- $\beta$ -CD inclusion complex and (d) TgC/HP- $\beta$ -CD physical mixture are shown in Fig. 8. Pure TgC appeared as irregular-shaped nanostructures with small dimensions, whereas HP- $\beta$ -CD showed typical amorphous spherical particles with cavity structures. The physical mixture of TgC/HP- $\beta$ -CD revealed some similarities with the Guest (TgC) and Host (HP- $\beta$ -CD) molecules and both crystalline and



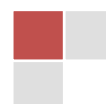
amorphous nature are quite visible. However, for the inclusion complex, the original morphology of TgC had completely disappeared, and it was impossible to differentiate the two components of TgC and HP- $\beta$ -CD, which lead to the conclusion of the formation of encapsulation complex.

### 3.8 Controlled release by fluorescence measurement:

In order to investigate the controlled release behaviour of the inclusion complex of the drug molecule, fluorescence experiment was done. Prior to the experiment, exact 100  $\mu$ M solution was prepared in distilled water and spectra were taken with different time. The result showed that the intensity of the solution was found to be decreasing up to 75 mins, then gradual increase in the intensity up to 150 mins. All the spectra were shown in Fig. S3 in supporting information. Fig. 9 showed a very good nature of the release profile and it suggested that HP- $\beta$ -CD can be used as sustained release drug carrier.

### 4. Conclusion:

In this present study, 1:1 inclusion complex of TgC and HP- $\beta$ -CD was prepared and various analytical techniques such as UV, NMR, and IR had been employed to Characterized the complex.  $^1\text{H}$ NMR and IR showed the mode of inclusion that N-methylated part of the pyridine ring was incorporated. Association constant value of the TgC/HP- $\beta$ -CD obtained by UV measurement was found to be  $-8416 \text{ M}^{-1}$  at 303K which indicate that interactions was very much negligible between guest and host and it was well matched with the value of  $-5000 \text{ M}^{-1}$  that obtained by fluorescence spectroscopy. It was the hydrogen bonding that was responsible for forming the encapsulation complex. Fluorescence measurement showed a well defined curve in intensity vs time kinetics and it gave us an idea about sustained release of the drug molecule from the encapsulated complex.

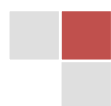


### **Acknowledgements:**

This work is highly appreciated by UGC SAP (special Assistant Programme) for giving us financial support for the completion of the work. Prof. M.N. Roy is very thankful to UGC-BSR (Basic Scientific Research) for awarding 'One Time Grant'. We would like to acknowledge Mr. Gautam Sarkar, USIC, Head, In-charge for taking SEM photograph and NEHU-SAIF for the NMR 400 MHz data acquisition.

### **Conflict of Interest:**

The authors declare no conflict of interest.



## TABLES

| Temp(K) | Ka/M <sup>-1</sup> | $\Delta H^0$<br>(KJ mol <sup>-1</sup> ) | $\Delta S^0$<br>(J mol <sup>-1</sup> K <sup>-1</sup> ) | $\Delta G$ KJ mol <sup>-1</sup> |
|---------|--------------------|---|--|---------------------------------|
| 293     | -141005.4          |   |  | -0.197                          |
| 298     | -69976.75          | 1.933                                   | 0.00727  | -0.234                          |
| 303     | -8416.58           |   |  | -0.270                          |

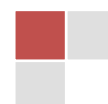
**Table 1: Data of the Van't Hoff equation for the calculation of thermodynamic parameters**

| Temp/K | Modified Stern–Volmer method |   |
|--------|------------------------------|---|
|        | Ka(M <sup>-1</sup> )         | Correlation Coefficient (R <sup>2</sup> ) |
| 308    | -5000                        | 0.923                                     |

**Table 2: Thermodynamic parameters for TgC and HP- $\beta$ -CD at 35 °C**

| TgC   | HP- $\beta$ -CD  | TgC/HP- $\beta$ -CD<br>inclusion                                       | TgC/HP- $\beta$ -CD<br>PHY MIX  |
|---|--|--|---|
| (I)3414 cm <sup>-1</sup> :<br>O-H from -COOH  | (I)3410 cm <sup>-1</sup> : $\nu$ (O-H)   | (I)3410 cm <sup>-1</sup> :<br>O-H from -COOH                           | (I)3400 cm <sup>-1</sup> :<br>O-H from -COOH                                      |
| (II)3084- 3040 cm <sup>-1</sup> :<br>C <sub>sp</sub> <sup>2</sup> -H from aromatic<br>Ring. | (II)2928 cm <sup>-1</sup> : $\nu$ (C <sub>sp</sub> <sup>3</sup> -H)                      | (II)2915 cm <sup>-1</sup> :<br>$\nu$ (C <sub>sp</sub> <sup>3</sup> -H) | (II)2927 cm <sup>-1</sup> :<br>$\nu$ (C <sub>sp</sub> <sup>3</sup> -H)            |
| (III)2357 cm <sup>-1</sup> :<br>C=N from aromatic<br>ring.                                  | (III)1635 cm <sup>-1</sup> : The OH groups in<br>the glucose moieties of HP- $\beta$ -CD | (III)2354 cm <sup>-1</sup> :<br>C=N from aromatic<br>ring.             | (IV)2356 cm <sup>-1</sup> :<br>C=N from<br>aromatic ring.                         |
| (IV)1711 cm <sup>-1</sup> :<br>-C=O from -COOH.   | (IV)1373 cm <sup>-1</sup> :<br>C-H from CH <sub>3</sub>                                  | (IV)1723 cm <sup>-1</sup> :<br>-C=O from -COOH.                        | (IV) 1701 cm <sup>-1</sup> :<br>-C=O from -<br>COOH.                              |
| (V)1469 and 1391<br>cm <sup>-1</sup> :<br>C=C double bond<br>from pyridine<br>moiety.       | (V)1152 cm <sup>-1</sup> :<br>Stretching frequency of C-O, C-C,<br>C-O-C.                |  | (V)1033 cm <sup>-1</sup> :<br>Bending<br>frequency of<br>O-C-H, C-C-H, C-<br>C-O. |
|   | (VI)1033 cm <sup>-1</sup> :<br>Bending frequency of<br>O-C-H, C-C-H, C-C-O.              |  |   |

**Table 3: Variation of the stretching frequencies (cm<sup>-1</sup>) of TgC and HP- $\beta$ -CD protons in free and complex states determined in KBr pellet**



## CHAPTER VI

| Trigonelline Hydrochloride                                      | HP- $\beta$ -CD | Inclusion Complex | Shift in HP- $\beta$ -CD proton |
|---|-----------------|-------------------|---------------------------------|
| (+)N-CH <sub>3</sub> : $\delta$ 4.321 (S, 3H)                   | H-1: 5.14       | H-1: 5.09         | -0.05                           |
| C <sub>2</sub> -H: $\delta$ 9.219 (S, 1H)                       | H-2: 3.50       | H-2: 3.56         | 0.02                            |
| C <sub>4</sub> -H: $\delta$ 8.857 - 8.814<br>(t, 1H, J ~7.2 Hz) | H-3: 3.90       | H-3: 3.86         | <b>-0.04</b>                    |
|   | H-4: 3.39       | H-4: 3.43         | -0.04                           |
| C <sub>5</sub> -H: $\delta$ 8.035 - 8.001<br>(t, 1H, J ~6.8 Hz) | H-5: 3.75       | H-5: 3.76         | <b>0.01</b>                     |
|   | H-6: 3.77       | H-6: 3.76         | -0.01                           |
| C <sub>6</sub> -H: $\delta$ 8.857 - 8.814<br>(t, 1H, J ~7.2 Hz) | Me: 1.03        | Me: 1.00          | -0.03                           |

**Table 4: Variation of the <sup>1</sup>H NMR chemical shifts ( $\delta$ /ppm) of TgC and HP- $\beta$ -CD protons in free and complex states determined in D<sub>2</sub>O**

| TgC(ml) | HP- $\beta$ -CD (ml) | TgC( $\mu$ M) | HP- $\beta$ -CD ( $\mu$ M) | [TgC]/([TgC]+[HP- $\beta$ -CD]) | Absorbance (A) | $\Delta A$ | $\Delta A^*[\text{TgC}]/([\text{TgC}]+[\text{HP-}\beta\text{-CD}])$ |
|---------|----------------------|---------------|----------------------------|---------------------------------|----------------|------------|---|
| 4       | 0                    | 100           | 0                          | 1                               | 0.64151        | 0          | 0   |
| 3.6     | 0.4                  | 90            | 10                         | 0.9                             | 0.58662        | 0.05489    | 0.049401  |
| 3.2     | 0.8                  | 80            | 20                         | 0.8                             | 0.5481         | 0.09341    | 0.074728  |
| 2.8     | 1.2                  | 70            | 30                         | 0.7                             | 0.50675        | 0.13476    | 0.094332  |
| 2.4     | 1.6                  | 60            | 40                         | 0.6                             | 0.47725        | 0.16426    | 0.098556  |
| 2       | 2                    | 50            | 50                         | 0.5                             | 0.44421        | 0.1973     | 0.09865   |
| 1.6     | 2.4                  | 40            | 60                         | 0.4                             | 0.4168         | 0.22471    | 0.089884  |
| 1.2     | 2.8                  | 30            | 70                         | 0.3                             | 0.3736         | 0.26791    | 0.080373  |
| 0.8     | 3.2                  | 20            | 80                         | 0.2                             | 0.39424        | 0.24727    | 0.049454  |
| 0.4     | 3.6                  | 10            | 90                         | 0.1                             | 0.26131        | 0.3802     | 0.03802   |
| 0       | 4                    | 0             | 100                        | 0                               | 0.37138        | 0.27013    | 0   |

**Table S1. UV Job's plot**

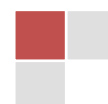


| Temp [TgC] | [HP-β-CD] |      |                |        |        |             |          |           |         |                    |
|------------|-----------|------|----------------|--------|--------|-------------|----------|-----------|---------|--------------------|
| /k         | (μM)      | (μM) | A <sub>o</sub> | A      | ΔA     | 1/[HPβCD]   | 1/ΔA     | Intercept | Slope   | Ka/M <sup>-1</sup> |
| 293        | 50        | 20   | 0.1033         | 0.0934 | 0.0099 | 50000       | 101.0101 |           |         |                    |
|            | 50        | 30   | 0.1033         | 0.0969 | 0.0064 | 33333.33333 | 156.25   |           |         |                    |
|            | 50        | 50   | 0.1033         | 0.0966 | 0.0067 | 20000       | 149.2537 | 174.8467  | 0.00124 | -141005.4          |
|            | 50        | 70   | 0.1033         | 0.0965 | 0.0068 | 14285.71429 | 147.0588 |           |         |                    |
|            | 50        | 80   | 0.1033         | 0.1096 | 0.0063 | 12500       | 158.7302 |           |         |                    |
| 298        | 50        | 20   | 0.0968         | 0.1147 | 0.0179 | 50000       | 55.86592 |           |         |                    |
|            | 50        | 30   | 0.0968         | 0.1108 | 0.014  | 33333.33333 | 71.42857 |           |         |                    |
|            | 50        | 50   | 0.0968         | 0.1102 | 0.0134 | 20000       | 74.62687 | 83.9721   | 0.0012  | -69976.75          |
|            | 50        | 70   | 0.0968         | 0.1101 | 0.0133 | 14285.71429 | 75.18797 |           |         |                    |
|            | 50        | 80   | 0.0968         | 0.1099 | 0.0131 | 12500       | 76.33588 |           |         |                    |
| 303        | 50        | 20   | 0.0953         | 0.0964 | 0.0011 | 50000       | 909.0909 |           |         |                    |
|            | 50        | 30   | 0.0953         | 0.0934 | 0.0019 | 33333.33    | 526.3158 |           |         |                    |
|            | 50        | 50   | 0.0953         | 0.0915 | 0.0038 | 20000       | 263.1579 | 181.7983  | 0.0216  | -8416.588          |
|            | 50        | 70   | 0.0953         | 0.1033 | 0.008  | 14285.71    | 125      |           |         |                    |
|            | 50        | 80   | 0.0953         | 0.1064 | 0.0111 | 12500       | 90.09009 |           |         |                    |

**Table S2. Association constant measurement by UV-vis measurement**

| TgC] | [HP-β-CD] | A <sub>o</sub> | A           | ΔA          | 1/[β-CD] | 1/ΔA        | Intercept | Slope    | Ka/M <sup>-1</sup> |
|------|-----------|----------------|-------------|-------------|----------|-------------|-----------|----------|--------------------|
| 50   | 20        | 456540.356     | 507886.8552 | 51346.49916 | 50000    | 1.94755E-05 |           |          |                    |
| 50   | 30        | 456540.356     | 553580.1462 | 97039.79018 | 33333.33 | 1.03051E-05 |           |          |                    |
| 50   | 50        | 456540.356     | 754072.4198 | 297532.0638 | 20000    | 3.36098E-06 | 2.00E-06  | 4.00E-10 | 5000               |
| 50   | 70        | 456540.356     | 638707.4866 | 182167.1306 | 14285.71 | 5.48946E-06 |           |          |                    |
| 50   | 80        | 456540.356     | 719868.4535 | 263328.0975 | 12500    | 3.79754E-06 |           |          |                    |

**Table S3: Association constant measurement by fluorescence measurement (303K)**



## CHAPTER VI

| Temp<br>(K) | Ka/M <sup>-1</sup> | 1/T         | lnKa    | Intercept | slope      | $\Delta H^0 /$<br>J mol <sup>-1</sup> | $\Delta S^0 /$<br>J mol <sup>-1</sup> K <sup>-1</sup> | $\Delta G^0 = (\Delta H^0 - T\Delta S^0)$<br>Jkmol <sup>-1</sup> | $\Delta G$ KJ mol <sup>-1</sup> |
|-------------|--------------------|-------------|---------|-----------|------------|---------------------------------------|---|--|---------------------------------|
| 293         | -141005.40         | 0.003412970 | 0.8434  |           |            |                                       |   | -197.6772375   | -0.197                          |
| 298         | -69976.75          | 0.0033557   | 0.08963 | 0.875     | -232.61933 | 95277.275                             | 1875  | -234.053175  | -0.234                          |
| 303         | -8416.58           | 0.003300330 | 0.11064 |           |            |                                       |   | -270.4291125   | -0.27                           |

**Table S4. Van't Hoff Plot Measurement**

| Vol. of<br>HP- $\beta$ -<br>CD(ml) | Total<br>Vol.(ml) | conc. Of TgC<br>(mM) | Conc. Of<br>HP- $\beta$ -CD<br>(mM) | Conc. Ratio of TgC & HP-<br>$\beta$ -CD | Conductivi<br>ty<br>(mSm <sup>-1</sup> ) |
|------------------------------------|-------------------|----------------------|-------------------------------------|---|--|
| 0                                  | 10                | 10                   | 0                                   | 0                                       | 18.2                                     |
| 1                                  | 11                | 9.909                | 0.0909                              | 0.009173479                             | 17.6                                     |
| 2                                  | 12                | 8.333                | 1.667                               | 0.200048002                             | 16                                       |
| 3                                  | 13                | 7.692                | 2.308                               | 0.300052002                             | 15.3                                     |
| 4                                  | 14                | 7.142                | 2.857                               | 0.400028003                             | 14.4                                     |
| 5                                  | 15                | 6.666                | 3.333                               | 0.5                                     | 13.6                                     |
| 6                                  | 16                | 6.25                 | 3.75                                | 0.6                                     | 12.9                                     |
| 7                                  | 17                | 5.882                | 4.118                               | 0.700102006                             | 12.3                                     |
| 8                                  | 18                | 5.555                | 4.444                               | 0.8                                     | 11.7                                     |
| 9                                  | 19                | 5.263                | 4.737                               | 0.900057002                             | 11.3                                     |
| 10                                 | 20                | 5                    | 5                                   | 1                                       | 10.8                                     |
| 11                                 | 21                | 4.761                | 5.239                               | 1.100399076                             | 10.4                                     |
| 12                                 | 22                | 4.545                | 5.455                               | 1.200220022                             | 10                                       |
| 13                                 | 23                | 4.347                | 5.653                               | 1.300437083                             | 9.7                                      |
| 14                                 | 24                | 4.166                | 5.834                               | 1.400384061                             | 9.42                                     |
| 15                                 | 25                | 4                    | 6                                   | 1.5                                     | 9.07                                     |
| 16                                 | 26                | 3.846                | 6.154                               | 1.600104004                             | 8.96                                     |
| 17                                 | 27                | 3.7                  | 6.3                                 | 1.702702703                             | 8.85                                     |
| 18                                 | 28                | 3.571                | 6.429                               | 1.80033604                              | 8.7                                      |
| 19                                 | 29                | 3.448                | 6.552                               | 1.900232019                             | 8.65                                     |
| 20                                 | 30                | 3.333                | 6.667                               | 2.00030003                              | 8.63                                     |
| 21                                 | 31                | 3.225                | 6.775                               | 2.100775194                             | 8.61                                     |

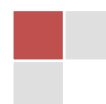
**Table S5. Conductance Measurement**

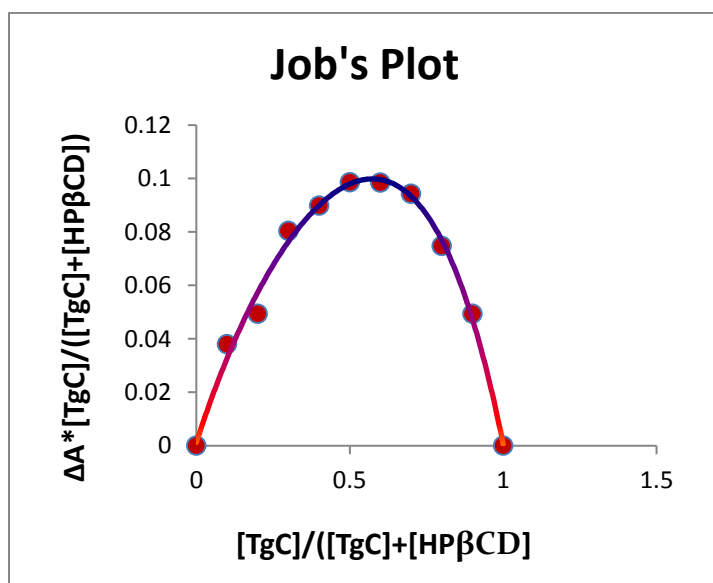


---

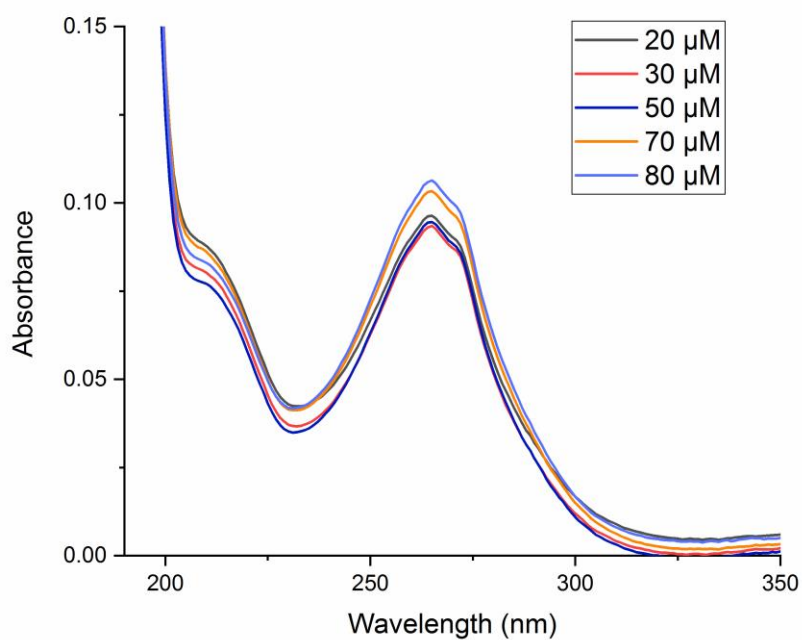
| Time (mins) | intensity |
|-------------|-----------|
| 0           | 53110.88  |
| 10          | 55688.60  |
| 20          | 51901.98  |
| 30          | 51628.77  |
| 40          | 49454.05  |
| 60          | 48544.78  |
| 75          | 45993.86  |
| 90          | 46122.63  |
| 105         | 47300.01  |
| 150         | 49666.18  |
| 210         | 44024.45  |

**Table S6. Release kinetics by fluorescence measurement**

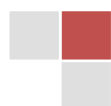


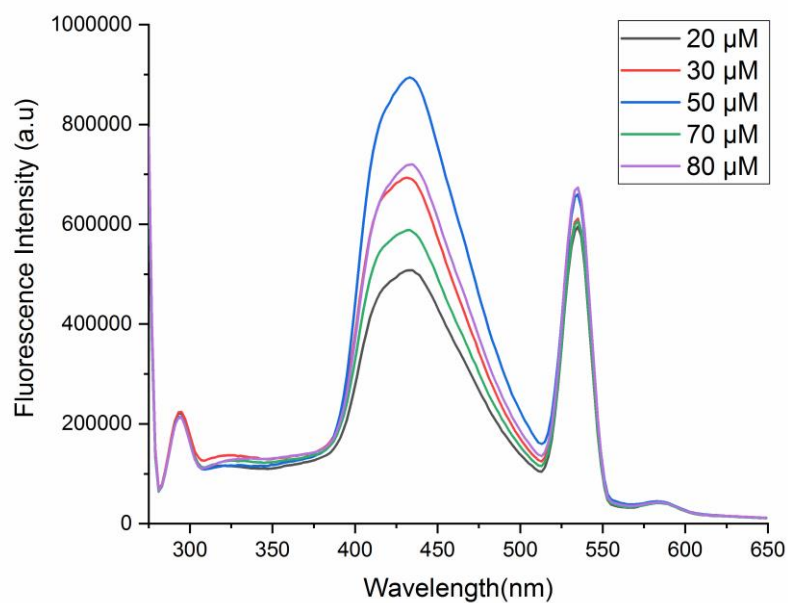
**FIGURES**

**Fig. 1: Job's plot of TgC/HP-β-CD**

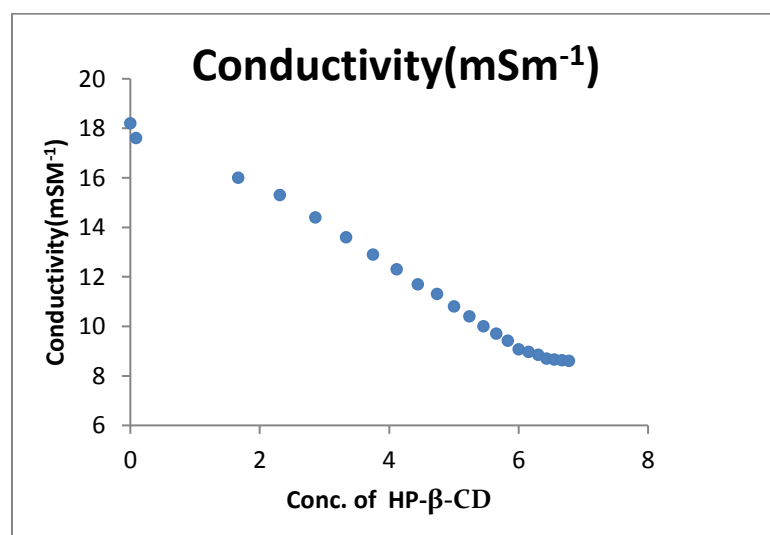


**Fig. 2: UV-vis spectral changes on addition of HP-β-CD where, different strength of the solution having 20 μM, 30 μM, 50 μM, 60 μM, 70 μM respectively were taken at 30°C**

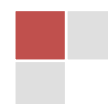




**Fig. 3: Variation in Fluorescence emission spectra of TgC and HP-β-CD in different molar concentration**



**Fig. 4: Plot of Specific conductivity vs conc. of HP-β-CD**



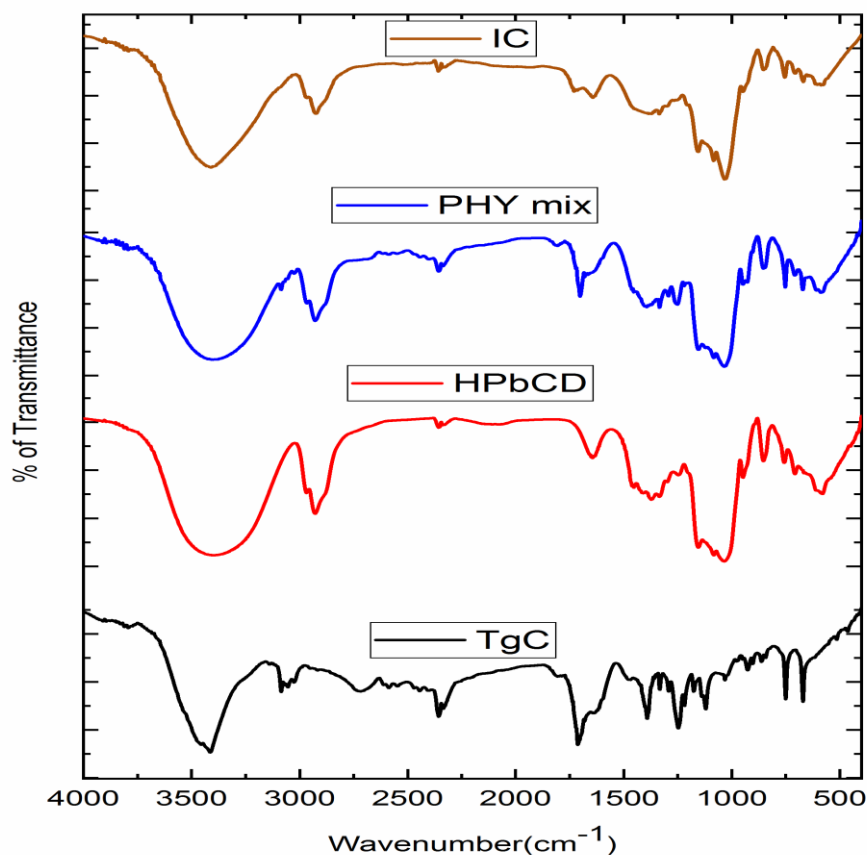


Fig. 5: FT-IR spectra of (a) TgC, (b) HP-β-CD (c) inclusion complex TgC/HP-β-CD (d) Physical mixture TgC/HP-β-CD

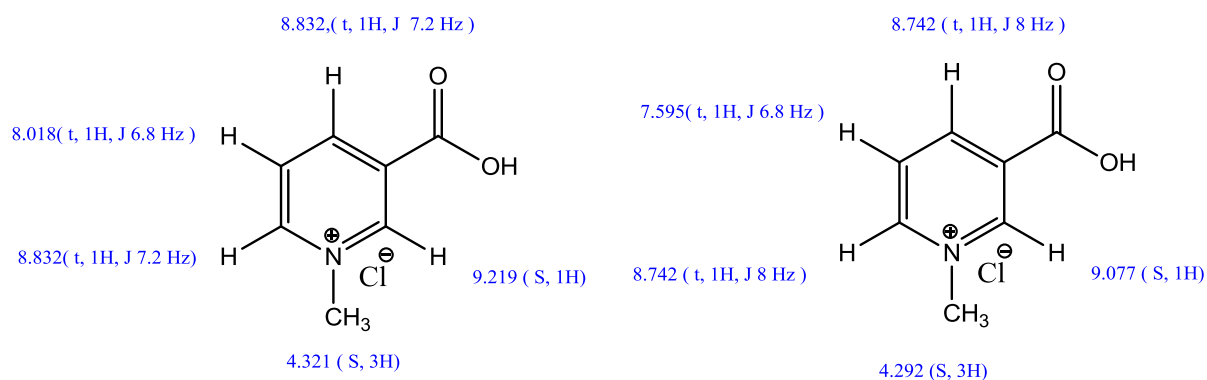


Fig. 6: Chemical Shift in NMR data of Free Trigonelline Hydrochloride (left) and after formation of encapsulation (right)



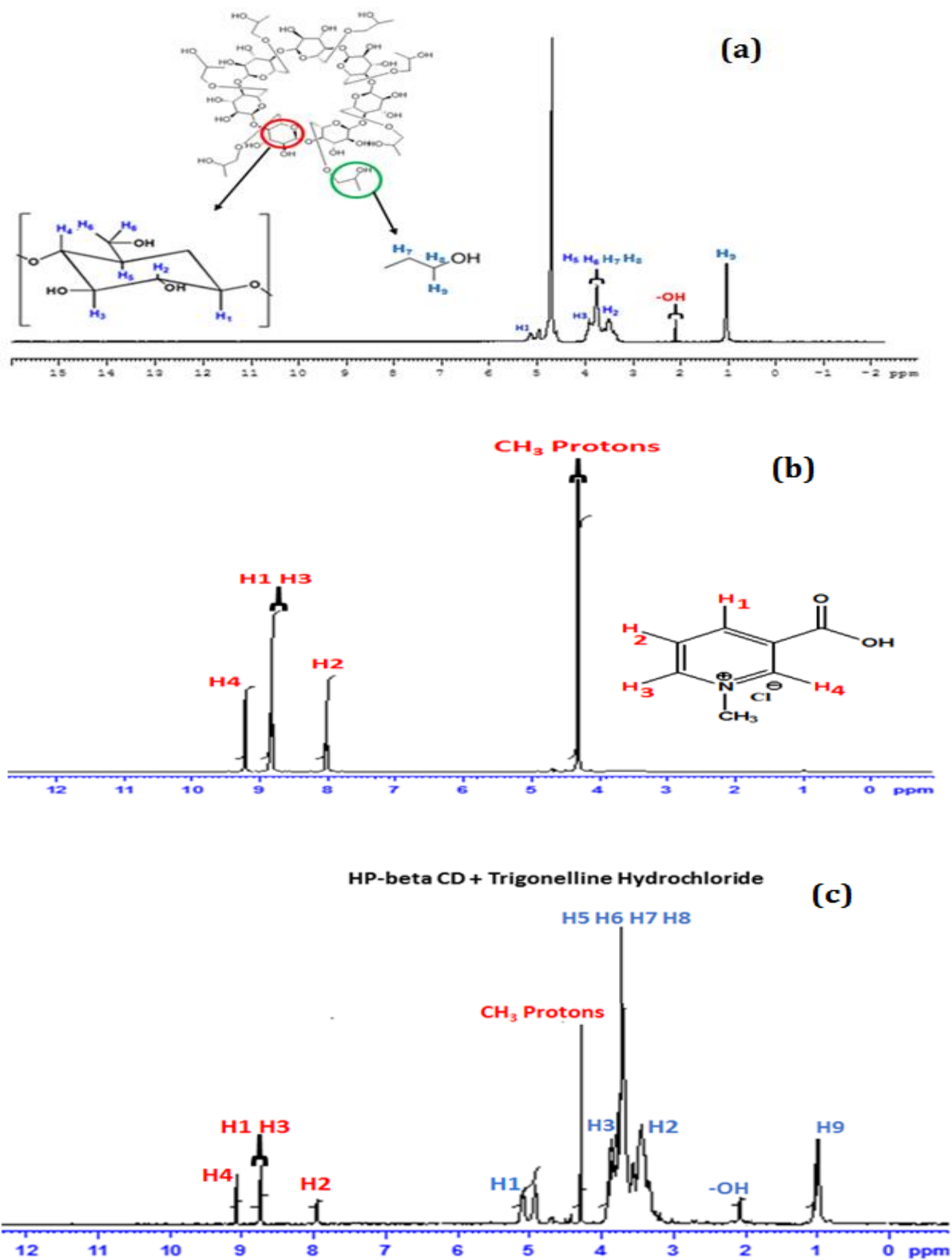
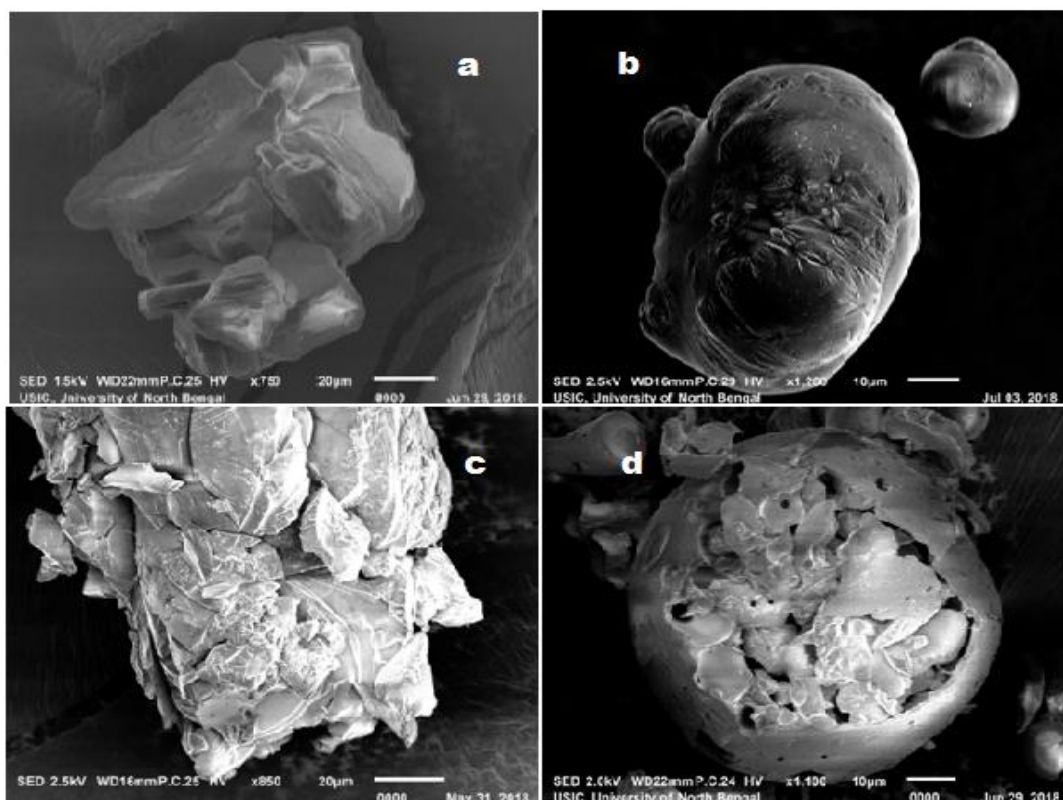
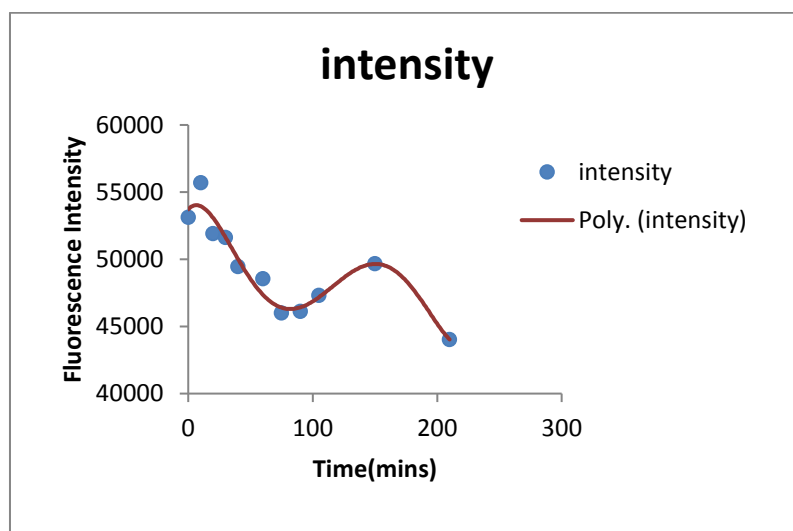


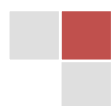
Fig. 7: NMR plot of (a) HP-β-CD (b) TgC (C) Inclusion complex TgC/HP-β-CD

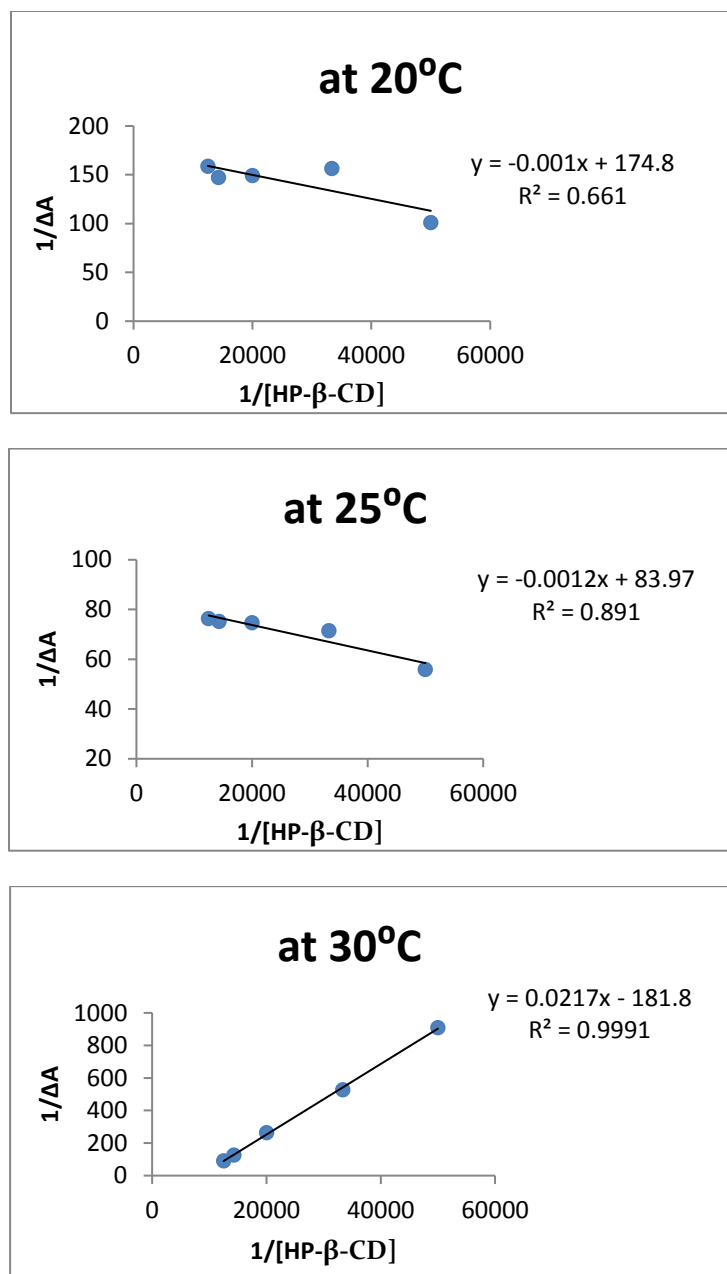


**Fig. 8: Scanning electron photograph for (a) TgC (b) HP-β-CD (c) TgC/ HP-β-CD inclusion complex (d) physical mixture**

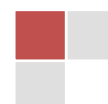


**Fig. 9: Schematic Drug release of TgC from Hydroxy propyl-β-Cyclodextrin**





**Fig. S1: Benesi-Hildebrand double reciprocal plot of TgC/HP-β-CD at three different temperatures**



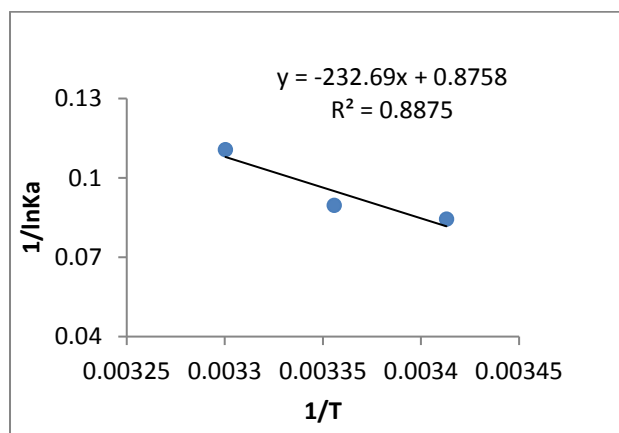


**Fig S2: Van't Hoff plot for the calculation of thermodynamic parameters ( $1/\ln K_a$  versus  $1/T$ )**

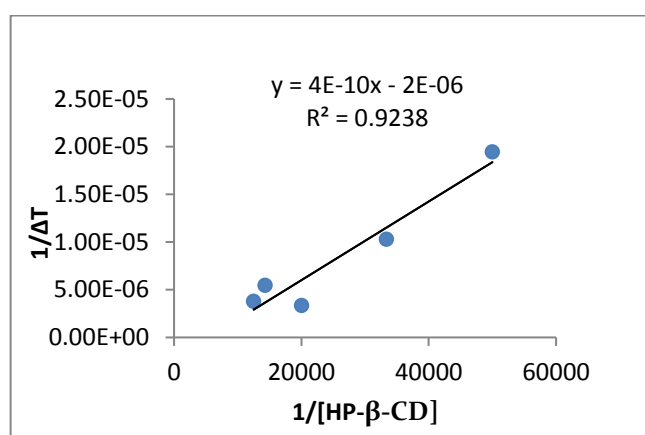


**Fig S3: Stern-Volmer plot for the effect of HP- $\beta$ -CD on the absorption of TgC**

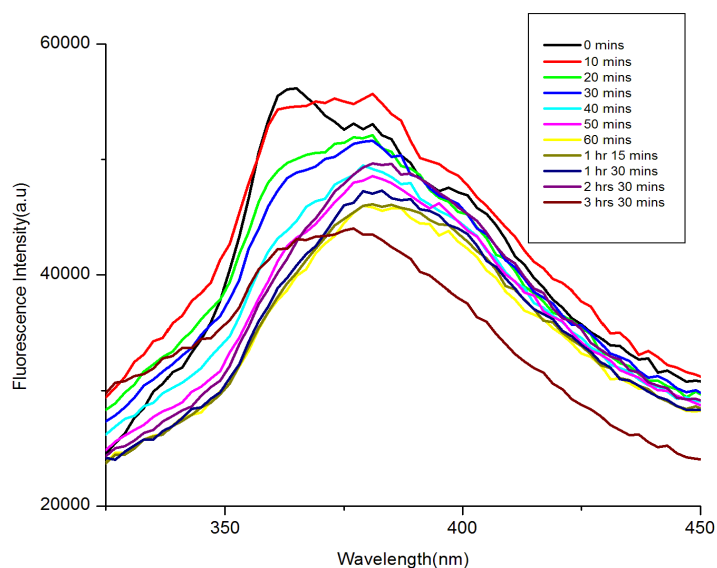
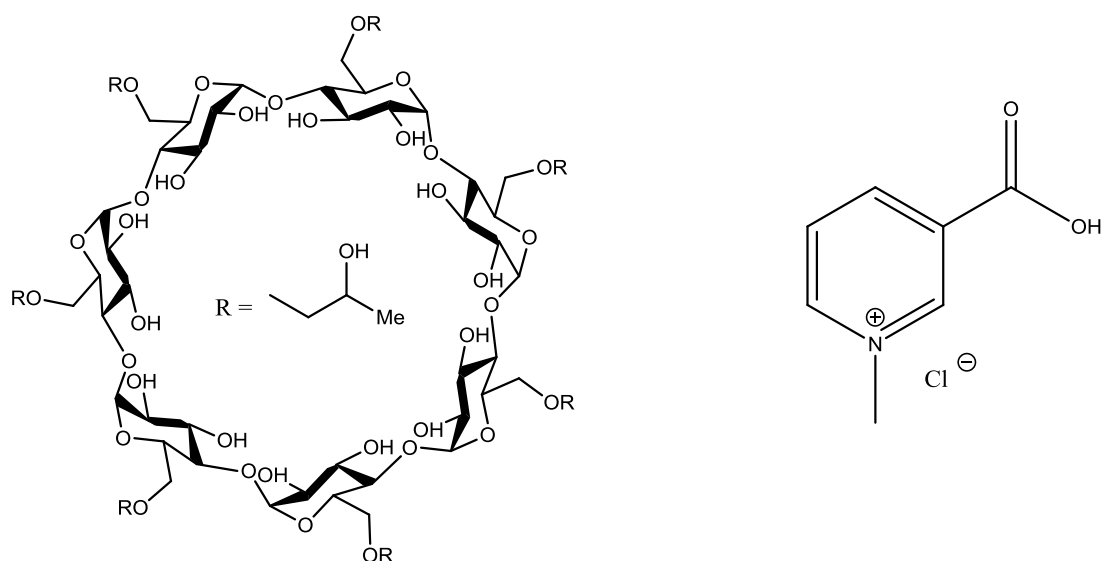


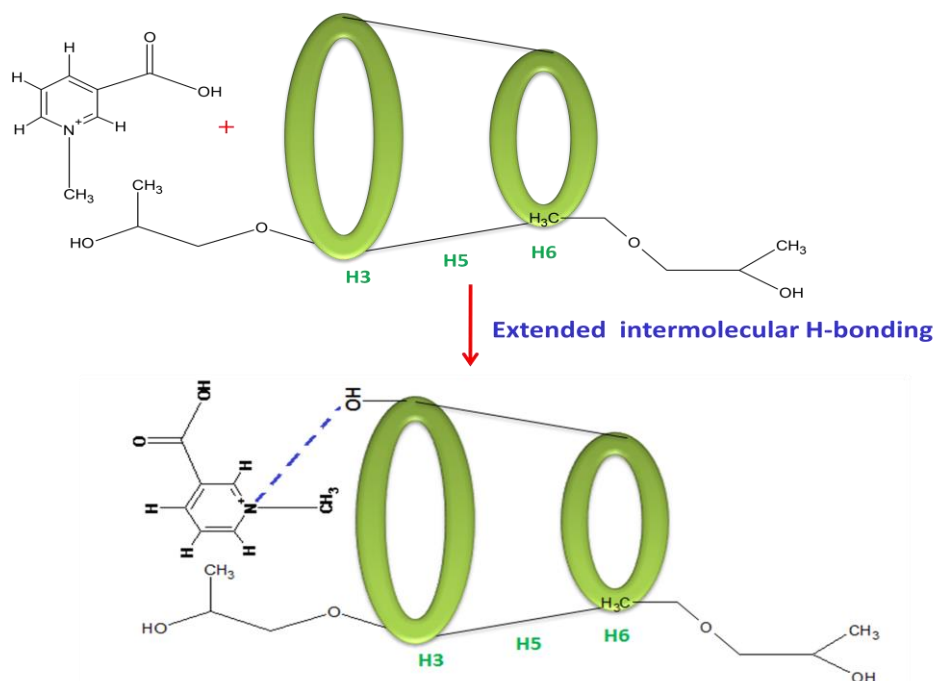
**Fig S4: Fluorescence spectra of inclusion complex with several time intervals**



## SCHEMES



**Scheme 1: The molecular structures of Hydroxypropyl beta cyclodextrin and Trigonelline hydrochloride.**



**Scheme 2: Schematic Representation for encapsulation**

